THE JOURNAL OF PHYSICAL CHEMISTRY A

Feature Article

Cite This: J. Phys. Chem. A 2019, 123, 8336−8348

pubs.acs.org/JPCA

Hydrogen-Bonding Mediated Reactions of Criegee Intermediates in the Gas Phase: Competition between Bimolecular and Termolecular Reactions and the Catalytic Role of Water

Wen Chao,[†] Cangtao Yin,[†] Kaito Takahashi,[†] and Jim Jr-Min Lin*[,†,‡]

[†]Institute of Atomic and Molecular Sciences, Academia Sinica, Taipei 10617, Taiwan

[‡]Department of Chemistry, National Taiwan University, Taipei 10617, Taiwan

Supporting Information

ABSTRACT: Criegee intermediates have substantial Zwitterionic character and interact strongly with hydrogen-bonding molecules like H_2O, NH_3, CH_3OH, etc. Some of the observed reactions between Criegee intermediates and hydrogen-bonding molecules exhibit third-order kinetics. The experimental data indicate that these termolecular reactions involve one Criegee intermediate and two hydrogen-bonding molecules; quantum chemistry calculation shows that one of the hydrogen-bonding molecules acts as a catalytic bridge, which receives a hydrogen atom and donates another one. In this Feature Article, we will discuss the roles of the hydrogen-bonding molecules and the trend of the reactivity for the title reactions. To better predict the competition between a catalyzed reaction (a termolecular process) and its bare reaction (a bimolecular process), we analyzed the free energy landscape of the competing reaction paths under pseudo-first-order conditions. The results indicate that the entropy reduction in the translational degrees of freedom is the main cause to hinder a catalyzed termolecular process under typical experimental concentrations at near ambient temperatures. For such a termolecular process to be significant, its energy gain (barrier lowering) by adding the catalytic molecule has to be large enough to compensate the corresponding entropy cost. One great advantage of this analysis is that the translational entropy only depends on simple parameters like temperature, reactant masses, and concentrations and thus can be easily estimated.

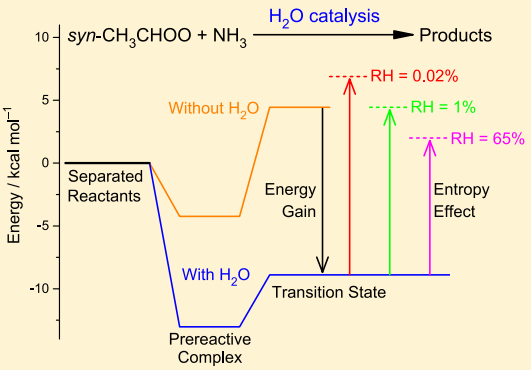

I. INTRODUCTION

Importance of Criegee Intermediates. Unsaturated hydrocarbons, including ethylene, propylene, isoprene, terpenes, etc., are emitted into our atmosphere in large quantities from both human and natural sources. Ozonolysis of unsaturated hydrocarbons forms highly reactive carbonyl oxides, through a reaction mechanism proposed by Rudolf Criegee.[1] Hence, the carbonyl oxide is also called a Criegee intermediate (CI). Criegee intermediates play important roles in atmospheric chemistry, including OH radical formation, oxidation of atmospheric molecules, including SO_2, NO_2, organic and inorganic acids, and even water.[2−5]

Novel Preparation Method of Criegee Intermediates. Due to the high reactivity and hence the short lifetime of Criegee intermediates, their steady-state concentrations are very low in most ozonolysis studies, and only indirect kinetic measurements have been performed. Because of the complicated reaction mechanisms, the reaction rate coefficients of Criegee intermediates that are deduced from these indirect kinetics measurements are often inconsistent and with large uncertainties of up to orders of magnitude.[6] In 2012, a new synthesis method was reported. For example, the simplest Criegee intermediate CH_2OO can be prepared by UV photolysis of CH_2I_2/O_2 mixture: $CH_2I_2 + h\nu \rightarrow CH_2I + I$; $CH_2I + O_2 \rightarrow CH_2OO + I$.[2] This novel method allows us to produce Criegee intermediates of high concentrations and high yields. Scientists can then directly measure the physical and chemical properties of Criegee intermediates.[7]

Zwitterionic Character and Structure-Dependent Reactivity. Both experimental and theoretical works have established that Criegee intermediates have strong Zwitterionic character with a large charge separation in the C═O—O functional group (positive C, negative terminal O).[8−10] In addition, the CO bond length is shorter than that of a typical CO single bond, indicating the CO bond is more like a double bond.[9] The rotation about the C═O double bond has a high barrier; thus, the *syn* and *anti* conformers of an asymmetrically substituted Criegee intermediate do not interconvert under typical experimental conditions.[11] Furthermore, due to the Zwitterionic character, the interaction of a Criegee intermediate with hydrogen-bonding (H-bonding) molecules is strong.

Received: July 25, 2019
Revised: September 7, 2019
Published: September 9, 2019

DOI: 10.1021/acs.jpca.9b07117
J. Phys. Chem. A 2019, 123, 8336−8348

Criegee intermediates of various structures have shown quite different reactivity. For example, CH_2OO and *anti*-CH_3CHOO react with water vapor very quickly,[12−14] but *syn*-CH_3CHOO and $(CH_3)_2COO$ react with water vapor more slowly.[13−15] On the other hand, *syn*-CH_3CHOO and $(CH_3)_2COO$ would undergo intramolecular hydrogen atom transfer from the CH_3 group at the *syn* position to the terminal oxygen;[16,17] this process may form OH radicals but is not the main unimolecular channel for CH_2OO and *anti*-CH_3CHOO.[18,19] Discussions on the physical and chemical properties of Criegee intermediates as well as their impacts on atmospheric chemistry can be found in a large number of publications, including a few review articles.[7,8,20,21]

Water-Mediated Reactions. Water is ubiquitous in the troposphere and its H-bonding interaction affects reactivity. Although a few theoretical works have suggested water enhancement in some atmospheric reactions,[22−30] experimental evidence is relatively sparse.[23,31] Only a limited number of atmospheric reactions exhibit significant water enhancement factors, defined as the ratio of the observed rate coefficients with and without the presence of water vapor[23] ($\lesssim$2.44 for HO_2 + HO_2, 1.96 for CH_3CHO + OH at 60 K, $\lesssim$ 1.67 for HO_2 + NO_2; see Table 2 of ref 23). To the best of our knowledge, large water enhancement (>10 times) of reactivity in atmospheric reactions has only been experimentally confirmed for reactions of SO_3 and Criegee intermediates.[32−36]

Water-Mediated Reactions Involving Criegee Intermediates. The reaction rate of CH_2OO with water vapor was found to depend on the square of the water concentration, suggesting the participation of two H_2O molecules.[4] Quantum chemistry calculations also indicate that the main reaction channel involves two H_2O molecules, which form a hydrogen-bonded chain with CH_2OO.[37−39] The calculated transition state (TS) energy (in this article, all TS energies are vibrational zero-point-energy (ZPE) corrected and relative to the infinitely separated reactants) is ca. 3 kcal mol^{-1} for the reaction CH_2OO + $1H_2O$; this energy is lowered by ca. 13 kcal mol^{-1} by adding one more H_2O molecule in the reaction system.[37−39] The product of the CH_2OO + $2H_2O$ reaction is hydroxymethyl hydroperoxide $(HO)CH_2OOH$,[40] the same as the expected product of the CH_2OO + H_2O reaction.[37−39] Thus, one of the two H_2O molecules can be considered as a catalyst.

Quantum chemistry calculations show that adding more water molecules would further decrease the TS energy. Indeed, the TS energy would further decrease by another 10.6 kcal mol^{-1} if we add another H_2O molecule to the $2H_2O$ system.[41] However, the two-water process predominates in the reaction of CH_2OO with water vapor when relative humidity (RH) is higher than 1% at 298 K, with no experimental evidence for the three-water process.[4,12,40]

Similar water-mediated reactions have been observed for the reactions of *anti*-CH_3CHOO + H_2O,[13] *syn*-CH_3CHOO + CH_3OH,[32] and *syn*-CH_3CHOO + NH_3.[33] Remarkably, the reaction of *syn*-CH_3CHOO + NH_3 shows an extraordinarily large water enhancement factor (138 at 278 K; 73 at 298 K) at near ambient conditions.[33] It appears that Criegee intermediates are special in terms of interactions with H-bonding molecules.

Main Question: Water Catalysis or Not? Bimolecular or Termolecular Reaction? For the above and similar reactions, quantum chemistry calculations often show lowering of the reaction barriers, which is partly due to the H-bonding induced by the additional water molecule.[22−30] But experimental results indicate that only some of such reactions exhibit water enhancement.[23,31,34] The question is how to predict whether there is water enhancement or not for a given reaction involving H-bonding. In a more general sense, water is just one of the H-bonding molecules. One may also ask about the effect of adding other H-bonding molecule (like CH_3OH, NH_3, etc.) to a given reaction system.

Water Enhancement in the Reaction CH_3CHO + OH at 60 K: A Hint of the Entropy Effect. In answering this question, we think it is important to look at the reaction CH_3CHO + OH. Vöhringer-Martinez et al.[31] have measured directly the reaction rates of OH with acetaldehyde in Laval nozzle expansions (a low temperature gas phase technique). Water enhancement (about a factor of 2) in the reaction rate could only be observed at a low temperature of ca. 60 K. The authors explained the lack of water enhancement at higher temperatures by the fact that water complexing with CH_3CHO is unfavorable at a higher temperature.[31] The water complexing is a process with a large entropy reduction, thus this finding suggests that the effect of entropy is important.

Our Approach: Consider the Entropy Cost ($\Delta G - \Delta E_0$). On the basis of the analyses on more than 10 reactions of Criegee intermediates with H-bonding molecules, we suggest considering the entropy reduction from the reactants to the transition state together with the energy lowering by including the additional catalytic molecule. Note that we will use the quantity of $\Delta G - \Delta E_0$ to represent the free energy change corresponding to the partition functions (G is the Gibbs free energy; E_0 is the energy at 0 K, which corresponds to the electronic energy including ZPE correction; Δ means the change from the reactants to the transition state or a complex). Under typical conditions, the entropy term $-T\Delta S$ is the main contributor of the $\Delta G - \Delta E_0$ term with a minor contribution of the thermal energy ΔE_{th} ($\Delta G = \Delta E_0 + \Delta E_{th} - T\Delta S$). See the Appendix for details. Although not rigorous, in this Feature Article, we still call this $\Delta G - \Delta E_0$ term as "entropy cost".

We further propose to draw a picture of the free energy landscape under a pseudo-first-order condition with relevant reactant concentrations, which allows us to link the energies from theoretical calculations with experimentally relevant observables like reaction rates. Note that although mathematically equivalent, this idea is a bit different from the conventional approach of considering the free energies at standard states (i.e., P = 1 bar for gaseous species).[42] For example, if one would like to consider the likelihood of water catalysis in the gas phase at ambient temperature, the use of the standard free energy of water vapor may be less convenient because the attainable partial pressure of water ($\lesssim$0.03 bar at 298 K) is much smaller than 1 bar.

How This Article Is Organized. In the following, first, we summarize the available experimental and theoretical kinetic data for four simple Criegee intermediates (CH_2OO, *anti*-CH_3CHOO, *syn*-CH_3CHOO, and $(CH_3)_2COO$) with three H-bonding molecules (H_2O, NH_3, and CH_3OH). Both bimolecular and termolecular processes are considered. Second, the TS energies of these reactions are analyzed. Third, we choose a few representative reactions to show the analysis of the entropy costs from the translational, rotational, and vibrational motions. Fourth, the free energy landscape is plotted together with the energy diagram to explain the

DOI: 10.1021/acs.jpca.9b07117
J. Phys. Chem. A 2019, 123, 8336−8348

observed reactivity trend. Finally, the water catalysis in other reaction systems and the remaining challenges are discussed.

II. REACTIVITY TREND

Figure 1 shows the Arrhenius plots for the bimolecular reactions of H_2O[13,18,32,38,43−45] (or NH_3[33,46−48]) with four simple Criegee intermediates. Note that for the reactions of CH_2OO and *anti*-CH_3CHOO with water vapor, the termolecular processes, which will be discussed in the next section, predominate at typical ambient conditions; here we discuss their bimolecular reactions first. In Figure 1, we can see that for the reactions with H_2O, CH_2OO and *anti*-CH_3CHOO are much more reactive than *syn*-CH_3CHOO and $(CH_3)_2COO$. In fact, the reactions of H_2O with *syn*-CH_3CHOO and $(CH_3)_2COO$ are too slow to measure (experimental data are not yet available).[13−15] There is a similar trend for the NH_3 reactions, among which the experimental rates of CH_2OO + NH_3 are much faster than those of *syn*-CH_3CHOO + NH_3.

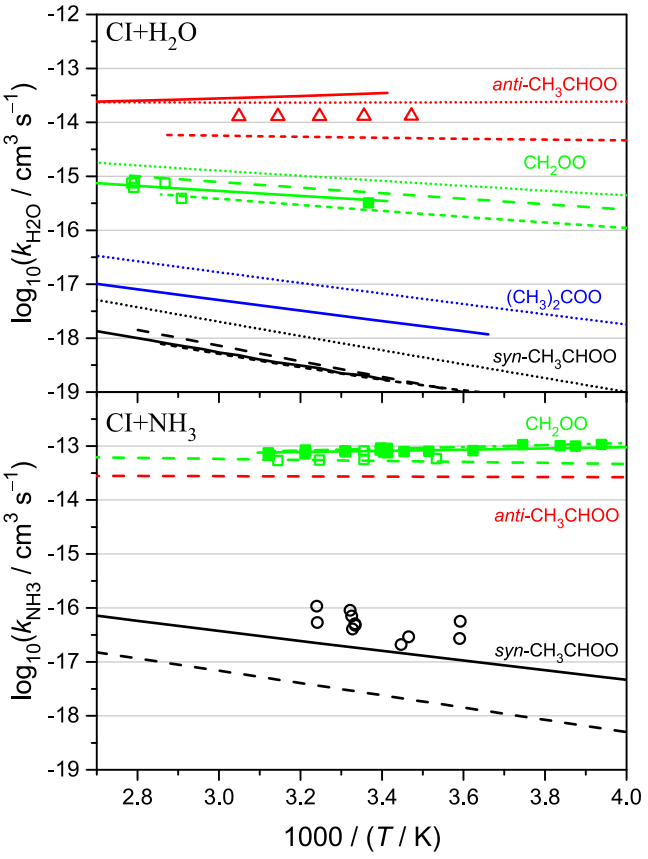

Figure 1. Arrhenius plots for the bimolecular reactions of H_2O (upper panel) and NH_3 (lower panel) with the four simple Criegee intermediates CH_2OO (green), *anti*-CH_3CHOO (red), *syn*-CH_3CHOO (black), and $(CH_3)_2COO$ (blue). The lines are the theoretical results. Upper panel: solid line, refs 38 and 43; short dashed line, ref 44; dashed line, ref 32; dotted line, ref 18. Lower panel: solid line, refs 33 and 46; dashed line, ref 47. The symbols of the corresponding colors are the experimental data. Upper panel: open triangle, ref 13; open square, ref 38; solid square, ref 45. Lower panel: open square, ref 46; solid square, ref 48; open circle, ref 33.

Figure 2 shows the Arrhenius plots for the termolecular reactions of the four simple Criegee intermediates with $2H_2O$[12,13,18,32,38,43] (or NH_3 + H_2O[33]). Under near ambient conditions, for example, 50% relative humidity (RH) and 298 K, the termolecular processes like CH_2OO + $2H_2O$, *anti*-CH_3CHOO + $2H_2O$, and *syn*-CH_3CHOO + NH_3 + H_2O, have been found as the dominant processes in the reaction systems. Similar to the bimolecular reactions discussed above, CH_2OO and *anti*-CH_3CHOO are more reactive than *syn*-CH_3CHOO and $(CH_3)_2COO$ for these termolecular reactions.

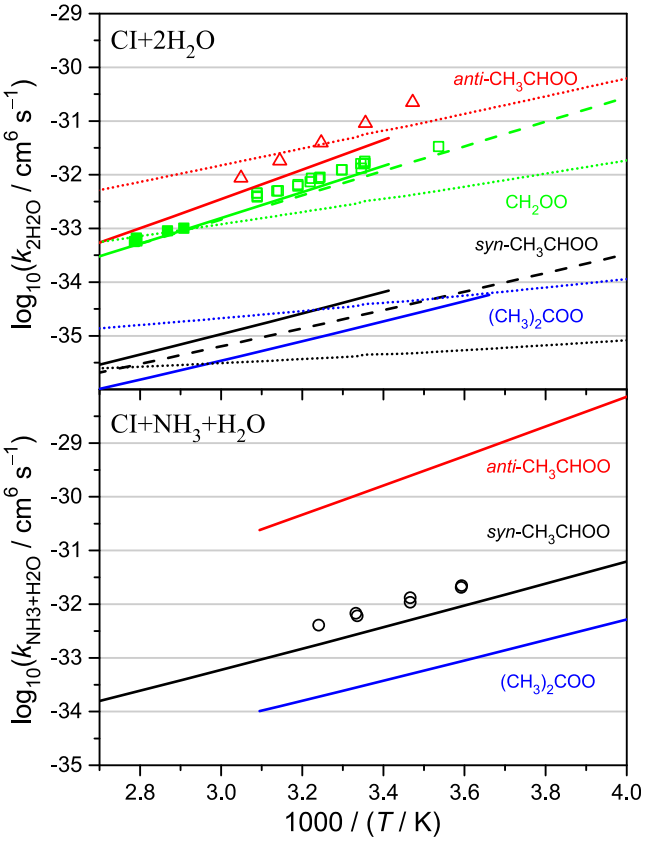

Figure 2. Arrhenius plots for the termolecular reactions of $2H_2O$ (upper panel) and NH_3 + H_2O (lower panel) with the four simple Criegee intermediates CH_2OO (green), *anti*-CH_3CHOO (red), *syn*-CH_3CHOO (black), and $(CH_3)_2COO$ (blue). The lines are the theoretical results. Upper panel: solid line, refs 38 and 43; dashed line, ref 32; dotted line, ref 18. Lower panel: ref 33 and this work. The symbols of the corresponding colors are the experimental data. Upper panel: open triangle, ref 13; open square, ref 38; solid square, ref 45. Lower panel: open circle, ref 33.

In this Feature Article, we analyzed the third-order kinetics as a termolecular reaction (like CI + NH_3 + H_2O) instead of a bimolecular reaction (like CI + $(H_2O)(NH_3)$). While these two analyses give the same results, we feel that the terminology of the termolecular reaction is more general and convenient. One of the reasons is that for the bimolecular description, there should be multiple types of bimolecular processes like $CI(NH_3)$ + H_2O, $CI(H_2O)$ + NH_3, etc.

For the systems with experimental data, the theoretical results often well reproduce the temperature dependences (similar slopes on the Arrhenius plots) and are also fairly consistent in terms of the absolute magnitude of the rate coefficients (within 0.5 orders of magnitude).

Figure 3 summarizes the kinetic data for CH_3OH reactions with Criegee intermediates.[32,49−52] CH_3OH shows higher reactivity than water, yet the trend of CH_3OH reactivity

DOI: 10.1021/acs.jpca.9b07117
J. Phys. Chem. A 2019, 123, 8336−8348

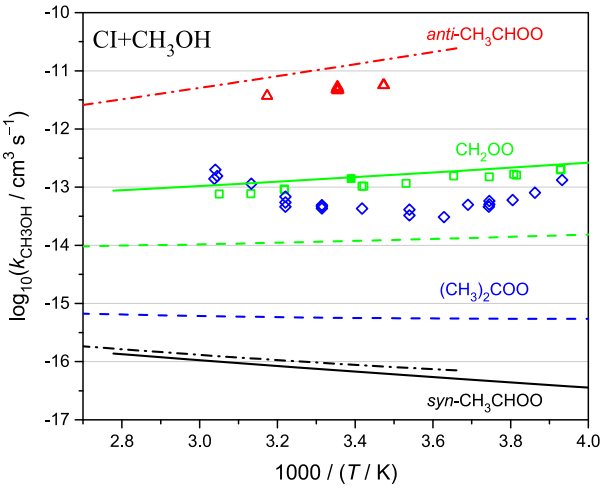

Figure 3. Arrhenius plots for the termolecular reactions of CH_3OH with the four simple Criegee intermediates CH_2OO (green), *anti*-CH_3CHOO (red), *syn*-CH_3CHOO (black), and $(CH_3)_2COO$ (blue). The lines are the theoretical results: solid line, ref 32; dashed line, ref 51; dash-dotted line, ref 50. The symbols of the corresponding colors are the experimental data: opened triangle, ref 50; open diamond and open square, ref 49; solid square, ref 52.

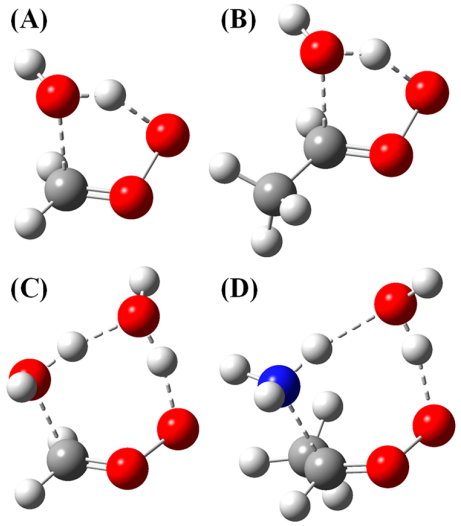

Figure 4. Schematic transition state geometries for the reactions of $CH_2OO + H_2O$ (A), *anti*-$CH_3CHOO + H_2O$ (B), $CH_2OO + 2H_2O$ (C), and *syn*-$CH_3CHOO + NH_3 + H_2O$ (D). The forming and breaking bonds are plotted as dashed lines. Element color code: C, gray; O, red; N, blue; H, white.

toward the four Criegee intermediates is similar to those of the H_2O and $2H_2O$ reactions.

Although the experimental reaction rates of $(CH_3)_2COO$ with CH_3OH are 2 orders of magnitude higher than the theoretical ones, the experimental results for the reactions with CH_2OO and *anti*-CH_3CHOO are in good agreement with the calculated rate coefficients.

Interestingly, previous experimental data indicate that the reaction of *syn*-CH_3CHOO with two CH_3OH molecules is the predominant reaction under typical laboratory conditions; the reaction with one CH_3OH cannot compete with the two CH_3OH reaction, unless at a high temperature (>323 K) or a low CH_3OH concentration ($<1 \times 10^{16}$ cm^{-3}).[50] All in all, the comparison between the experimental and computational results gives us confidence to evaluate the reactivity of simple Criegee intermediates using the results from credible theoretical approaches.

III. TS GEOMETRIES AND ENERGIES: GENERAL FEATURES

Figure 4 shows the transition-state geometries for the reactions of $CH_2OO + H_2O$,[38] *anti*-$CH_3CHOO + H_2O$,[38] $CH_2OO + 2H_2O$,[38] and *syn*-$CH_3CHOO + NH_3 + H_2O$[33] as typical examples for the title reactions. We can see that these transition state structures have common features: (i) All involve H-bonding. (ii) All involve a proton (or H atom) transfer to the terminal oxygen and a nucleophilic attack to the carbonyl carbon of the Criegee intermediate. (iii) For the $2H_2O$ and $NH_3 + H_2O$ reactions, one H_2O molecule acts as a bridge that accepts a proton and releases another proton. Here we refer to this bridging molecule, which is regenerated after the reaction, as a **catalyst**. For the reaction of *syn*-$CH_3CHOO + NH_3 + H_2O$, the NH_3 can also act as the bridging molecule, but this channel has a significantly higher transition state energy (Table 1 and Figure 5). Similar mechanisms have been reported for *syn*-$CH_3CHOO + CH_3OH + H_2O$[32] and *syn*-$CH_3CHOO + 2CH_3OH$.[50] The barrier lowering by including the bridge molecule may be rationalized by considering the frontier molecular orbitals of a Criegee intermediate, which is a π system consisting of three atomic p-orbitals perpendicular to the COO plane. If there is only one H-bonding molecule (as in Figure 4A/B), the nucleophilic attack and proton transfer cannot reach the optimal conditions of orbital overlap simultaneously due to the geometry constraint. The addition of the second H-bonding molecule releases this constraint by acting as a proton transfer bridge[33] (as in Figure 4C,D).

Role of Tunneling. At first sight, it seems that tunneling should be important for the title reactions. However, previous studies by our group,[38,53] by Anglada et al.,[39] and by Truhlar and co-workers[44] have shown that the tunneling effect is weak at near 298 K, very different from the cases of intramolecular H atom transfer reactions for *syn*-CH_3CHOO and $(CH_3)_2COO$.[16,17] This is because proton transfer is only a part of the reaction; the nucleophilic attack also has to occur. For reactions of *syn*-CH_3CHOO with $2CH_3OH/2CH_3OD$, a kinetic isotope effect of ~2.5 (~4) was found experimentally (computationally), but this was attributed to the differences in vibrational zero-point energies and in partition functions rather than to tunneling.[50] For reactions of $(CH_3)_2COO$ with methanol, no significant effects were observed among various isotopologues of the methanol reactants.[49]

Tight Submerged Barrier. For a termolecular reaction A + B + C → products, in which the reactants may form dimeric H-bonding complexes, we may picture the whole reaction as the sum of the contributions of various reaction pathways, such as AB + C, AC + B, and A + BC. The AB + C path is exemplified below.

$$A + B \leftrightarrow AB$$

$$AB + C \leftrightarrow ABC^{\dagger} \rightarrow \text{products}$$

$$AB + C \leftrightarrow ABC \leftrightarrow ABC^{\dagger} \rightarrow \text{products}$$

where a bound dimer AB is formed by association of A and B; the reaction of AB with the third reactant C may reach the transition state ($ABC^{\dagger}$) either by direct means or via a bound trimer ABC; then the products are formed through $ABC^{\dagger}$.

DOI: 10.1021/acs.jpca.9b07117
J. Phys. Chem. A 2019, 123, 8336−8348

Table 1. Energy of the Transition State (kcal mol^{-1}) Relative to the Infinitely Separated Reactants[a]

	CH_2OO	*anti*-CH_3CHOO	*syn*-CH_3CHOO	$(CH_3)_2COO$
H_2O	2.82[b,38]	0.34[b,38]	6.96[b,38]	5.35[b,43]
	3.48[c,44]	1.18[c,44]	7.53[c,44]	
	1.5[d,39]	−1.2[d,39]	5.34[d,39]	3.57[d,39]
	2.81[b,32]		6.96[b,32]	
CH_3OH	−2.07[b,32]	−4.87[b,50]	1.91[b,50]	
	−0.91[e,51]	−4.24[e,51]	2.4[e,51]	0.29[e,51]
	−0.91[f,49]		1.91[b,32]	0.29[f,49]
	−2.9[g,52]			
NH_3	−0.44[b,46]	−0.82 (this work)[b]	4.44[b,33]	4.48 (this work)[b]
	0.42[h,47]	0.09[h,47]	5.20[h,47]	
	−0.65[i,48]			
$2H_2O$	−9.43[b,38]	−10.56[b,38]	−6.32[b,38]	−6.26[b,43]
	−11.4[d,39]	−12.85[d,39]	−8.78[d,39]	−8.96[d,39]
	−9.44[b,32]		−6.32[b,32]	
$2NH_3$	−8.86 (this work)[b]	−8.06 (this work)[b]	−4.52[b,33]	−3.4 (this work)[b]
$2CH_3OH$	−16.91[b,32]		−14.72[b,50]	
$NH_3 + H_2O$ (H_2O cat.)	N.A.[j]	−12.22 (this work)[b]	−8.89[b,33]	−8.09 (this work)[b]
$H_2O + NH_3$ (NH_3 cat.)	−7.39 (this work)[b]	−7.36 (this work)[b]	−3.25[b,33]	−2.24 (this work)[b]
$CH_3OH + H_2O$ (H_2O cat.)	−14.75[b,32]		−12.24[b,32]	
$H_2O + CH_3OH$ (CH_3OH cat.)	−11.84[b,32]		−8.86[b,32]	

[a]All the values are corrected for the vibrational zero-point energy. [b]Calculated at QCISD(T)/CBS//B3LYP/6-311+G(2d,2p), including ZPE correction at B3LYP/6-311+G(2d,2p). CBS means extrapolation to the complete basis set limit using Dunning's correlation consistent double, triple, and quadruple-ζ basis sets. [c]Calculated at the W3X-L//QCISD/cc-pVTZ level. [d]Calculated at CCSD(T)/aug-cc-pVTZ//B3LYP/6-311+G(2df,2p), including ZPE correction at B3LYP/6-311+G(2df,2p). [e]Calculated at DF-LCCSD(T)-F12a/aug-cc-pVTZ//B3LYP/aug-cc-pVTZ, including ZPE correction at B3LYP/aug-cc-pVTZ. [f]Calculated at DF-LCCSD(T)-F12a/aug-cc-pVTZ//B3LYP/aug-cc-pVTZ with thermodynamic corrections from the B3LYP/aug-cc-pVTZ vibrational frequency analysis. [g]Calculated at the CCSD(T)/aug-cc-pVDZ//CCSD/cc-pVDZ level of theory. [h]Calculated at CCSD(T)/CBS//CCSD(T)/ANO2 (or CCSD(T)/CBS//CCSD(T)/ANO1 for CH_2OO) with perturbative quadruples corrections. [i]Calculated at the CCSD(T)(F12*)/cc-pVQZ-F12//CCSD(T)(F12*)/cc-pVDZ-F12 level. [j]No barrier can be found on the electronic energy surface.

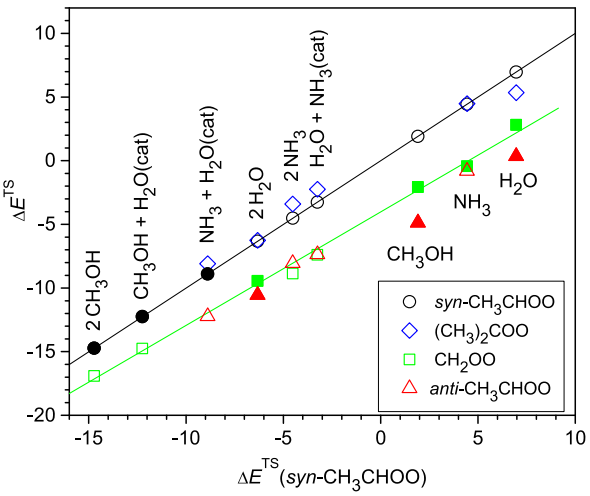

Figure 5. Correlation of the TS energies (QCISD(T)/CBS//B3LYP/6-311+G(2d,2p), ZPE correction at B3LYP/6-311+G(2d,2p) in Table 1) of the reactions of the four Criegee intermediates (green square, red triangle, black circle, blue diamond symbols to represent CH_2OO, *anti*-CH_3CHOO, *syn*-CH_3CHOO, and $(CH_3)_2COO$, respectively) with the considered coreactants (H_2O, NH_3, CH_3OH, and their catalytic combinations). The horizontal axis is the TS energies of the reactions of *syn*-CH_3CHOO. The black line is the diagonal line to guide the eye; the green line is the linear fit to the TS energies of the reactions of CH_2OO. The reactions that have been reported as the dominant ones are indicated by filled symbols.

In the reactions of a Criegee intermediate with two H-bonding molecules, the energy of ABC† is often submerged (lower than that of AB + C). To treat such a case theoretically, a two-transition-state model has been reported in the literature.[54,55] It suggests that both the addition process (AB + C ↔ ABC) and the reactive process (ABC† → products) may limit the overall rate. However, for the reactions studied in this Feature Article, previous works (mentioned in Table 1) suggest that ABC† has a tight structure and the overall reaction rate is mainly limited by the passage through ABC†; in addition, the reaction rates are calculated by assuming that ABC is in equilibrium with A, B, and C. Thus, the overall termolecular reaction rate coefficient k_{3M} can be expressed as $k_{3M} = K_{eqABC}k_{uni}$, where K_{eqABC} is the equilibrium constant for A + B + C ↔ ABC and k_{uni} is the unimolecular rate coefficient of ABC ↔ ABC† → products. The energy and partition functions of ABC appear in both K_{eqABC} and k_{uni}, but they are canceled out in the final expression of k_{3M}, which only depend on the properties of ABC† and the reactants A + B + C. Therefore, we mainly discuss the differences between ABC† and A + B + C in this Feature Article. Similarly, for another picture of A + B + C ↔ AB + C ↔ ABC† → products, the overall rate coefficient can also be expressed as $k_{3M} = K_{eqAB}k_{AB+C}$ and k_{3M} also only depends on ABC† and A + B + C under the equilibrium assumption.

Comments on Quantum Chemistry Methods. In Table 1, most previous studies have used density functional theory methods to obtain the geometries and vibrational frequencies. The electronic energies are usually refined at CCSD(T) or QCISD(T). Some studies included explicitly correlated F-12 methods and usually the core electrons are left out in the correlation calculation. It is beyond our scope to evaluate various methods, but we comment on the method that we have

DOI: 10.1021/acs.jpca.9b07117
J. Phys. Chem. A 2019, 123, 8336−8348

used, which is a complete basis set extrapolation of QCISD(T)[56] energies using Dunning's aug-cc-pVDZ, aug-cc-pVTZ, and aug-cc-pVQZ basis sets[57−59] at the geometries calculated at B3LYP/6-311+G(2d,2p).[60,61] For the CH_2OO + H_2O and CH_2OO + $2H_2O$ reactions, we have also calculated the TS geometries using QCISD(T)/aug-cc-pVTZ, and found that the use of B3LYP geometries can cause variations of ∼0.2 kcal mol^{-1} in the TS energies.[38] In addition, we should mention that the T1 diagnostic values for Criegee intermediates are not small (∼0.05), suggesting multireference character. For the CH_2OO + H_2O reaction, we have seen that multireference configuration interaction with Davidson's correction (MRCI+Q (10 *e*,10 *o*)) can give TS energies that are ∼1 kcal mol^{-1} higher than those obtained by QCISD(T).[38]

Trend of the TS Energy. We compiled the available TS energies for the reactions involving H_2O, CH_3OH, NH_3 with four simple Criegee intermediates in Table 1. We can see that the results from different groups are quite consistent. In Figure 5, we compare these transition state energies for the four simple Criegee intermediates (CH_2OO, *anti*-CH_3CHOO, *syn*-CH_3CHOO, and $(CH_3)_2COO$) with three coreactants (H_2O, NH_3, and CH_3OH). Both bimolecular and termolecular processes are considered. We can see that there are strong correlations among the TS energies for the four Criegee intermediates with a trend of ΔE^{TS}(*anti*-CH_3CHOO) ≈ $\Delta E^{TS}(CH_2OO)$ < ΔE^{TS}(*syn*-CH_3CHOO) ≈ $\Delta E^{TS}((CH_3)_2COO)$. Some deviations (2−3 kcal mol^{-1}) are found for the reactions of $1H_2O$ and $1CH_3OH$, of which ΔE^{TS}(*anti*-CH_3CHOO) is extraordinarily lower than $\Delta E^{TS}(CH_2OO)$. A second observation is that, for the coreactants, CH_3OH has a lower barrier than NH_3; NH_3 has a lower barrier than H_2O. A similar trend is found for the reactions involving $2CH_3OH$, $2NH_3$, and $2H_2O$.

It is expected that a lower TS energy is correlated with a faster rate for reactions of similar mechanism. The reactions of *syn*-CH_3CHOO with $2CH_3OH$, CH_3OH + H_2O, and NH_3 + H_2O have been found to be very efficient.[32,33,50] However, while the kinetics of the CH_2OO+NH_3 reaction has been reported by a few groups,[46,48] there is no experimental evidence for the CH_2OO + $2NH_3$ reaction yet. At first, this seems strange considering that the latter has a lower ΔE^{TS} = −8.86 kcal mol^{-1} than the former (ΔE^{TS} = −0.44 kcal mol^{-1}). Considering that these two reactions have different reaction orders, one should be able to differentiate them experimentally. At low [NH_3], the second-order CH_2OO + NH_3 reaction would predominate over the third-order CH_2OO + $2NH_3$ reaction and at higher [NH_3], one would expect the CH_2OO + $2NH_3$ reaction to contribute. This has been observed for the case of *anti*-CH_3CHOO reaction with water vapor at room temperature, where the reaction of one water molecule dominates at low [H_2O], and the reaction with two water molecules becomes dominant at high [H_2O].[13,14] We also note that at lower temperatures, the contribution of the reaction involving two water molecules becomes larger.[13] But to know what NH_3 concentration is high enough to observe the third-order reaction, it would require the corresponding rate coefficients. Unfortunately, some theoretical works[22−27] only compute the reaction barriers without providing the rate coefficients. Under this circumstance, it may be hard for an experimentalist to "guess" which reaction (second order or third order) would predominate.

Considering the main difference between bimolecular and termolecular processes, we can imagine that there is a lower probability to bring three reactant molecules together than to bring two. That is, the entropy reduction of a reaction system to reach a termolecular transition state is much more significant than that to reach a bimolecular one. As will be shown below, we think it would be useful to analyze the corresponding entropy "cost" of the processes of interest, which might offer a simpler way to answer the above question.

IV. ANALYSIS OF THE REACTION RATES IN TERMS OF THE FREE ENERGY CHANGE AND THE ENTROPY COST

To compare the effects of competing reactions of different orders, scientists often use pseudo-first-order rate coefficients as the effective quantities. In Figure 6, we adopted a similar approach to plot the pseudo-first-order rate coefficients k_{eff} of *syn*-CH_3CHOO at given [H_2O] and [NH_3]. Here we artificially set [NH_3] = 5 × 10^{17} cm^{-3}, which is about a medium value in our previous experiments.[33] Note that since the two reactions under consideration both have one NH_3 molecule on the reactant side, the choice of [NH_3] would not affect their competition. Although k_{eff} (as a function of [H_2O] and [NH_3]) would already give the needed information about the kinetics of the reaction system, we also like to convert k_{eff} to a scale of free energy by using the conventional transition state theory (see Appendix), such that the effects of the partition functions and reactant concentrations can be viewed on the energy scale and we can further see the effect of the potential energy more directly. The resulting free energy change ($\Delta G^{1st\text{-}ord}$) is shown on the left axis of Figure 6 for two exemplified bimolecular and termolecular processes, the reaction of *syn*-CH_3CHOO + NH_3 and its water catalyzed variant.

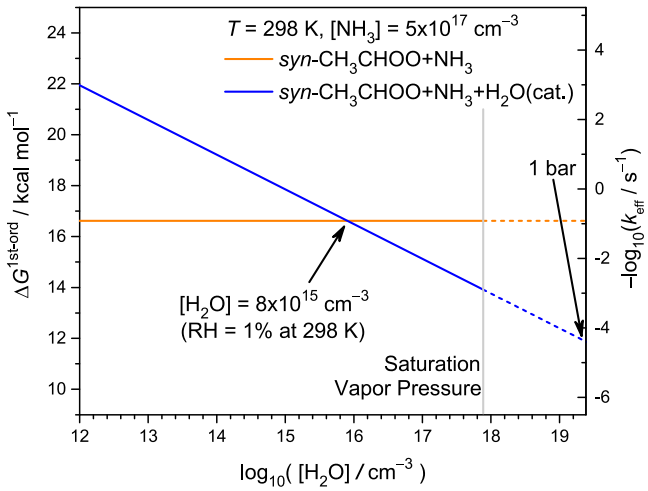

Figure 6. Theoretical pseudo-first-order rate coefficients of k_{eff} (right axis) of the reactions of *syn*-CH_3CHOO + NH_3 and *syn*-CH_3CHOO + NH_3 + H_2O (H_2O catalyzed channel) as a function of [H_2O] at [NH_3] = 5 × 10^{17} cm^{-3}. On the basis of the conventional transition state theory, we convert k_{eff} to the corresponding Gibbs free energy changes from the reactants to the transition states (left axis). The saturation vapor pressure of H_2O at 298 K is marked as a gray vertical line. Results are from the energies calculated by QCISD(T)/CBS//B3LYP/6-311+G(2d,2p) and partition functions calculated with rigid-rotor-harmonic-oscillator model at B3LYP/6-311+G(2d,2p). See Tables S5−S10 for the parameters used to calculate the partition functions in this work.

DOI: 10.1021/acs.jpca.9b07117
J. Phys. Chem. A 2019, 123, 8336−8348

For the bare reaction, *syn*-CH_3CHOO + NH_3, which does not involve H_2O, $\Delta G^{1st\text{-}ord}$ and k_{eff} are of course a flat line. For the water catalyzed reaction, $\Delta G^{1st\text{-}ord}$ shows a linear relationship when plotted against $\log_{10}([H_2O])$. While Figure 6 only shows the expected results of the conventional transition state theory, it allows us to view the competition between the two processes very directly. For example, the $\Delta G^{1st\text{-}ord}$ of the termolecular process becomes lower at higher $[H_2O]$ and it starts to dominate at relative humidity RH > 1%. Note that there is a significant difference of ca. 5 kcal mol^{-1} in $\Delta G^{1st\text{-}ord}$ from RH = 1% to the hypothetical standard state (P = 1 bar).

In Figure 7, we compare the entropy costs, $\Delta G^{1st\text{-}ord} - \Delta E_0$, from the reactants to the transition states for five processes of

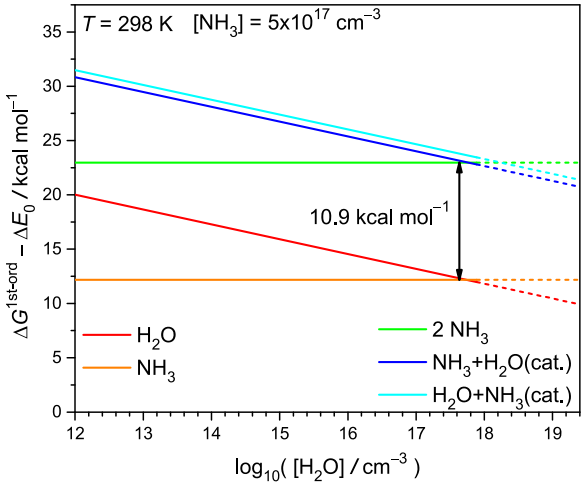

Figure 7. Entropy cost ($\Delta G^{1st\text{-}ord} - \Delta E_0$) from the reactants to the transition states for the reactions of *syn*-CH_3CHOO + NH_3, *syn*-CH_3CHOO + H_2O, and *syn*-CH_3CHOO + NH_3 + H_2O (both the H_2O-catalyzed and NH_3-catalyzed channels) as a function of $[H_2O]$ at a fixed $[NH_3] = 5 \times 10^{17}$ cm^{-3}. The dashed lines show the region that $[H_2O]$ is larger than the saturation vapor pressure. The calculation method is the same as that of Figure 6.

the *syn*-CH_3CHOO reactions at a fixed $[NH_3] = 5 \times 10^{17}$ cm^{-3} and various $[H_2O]$. Note, as detailed in the Appendix, $\Delta G^{1st\text{-}ord} - \Delta E_0 = \Delta E_{th} - T\Delta S$ and $|\Delta E_{th}| \ll |T\Delta S|$ under typical conditions; thus, the entropy term $-T\Delta S$ comprises the major part of $\Delta G^{1st\text{-}ord} - \Delta E_0$. For the two bimolecular processes (*syn*-CH_3CHOO + H_2O and *syn*-CH_3CHOO + NH_3), their entropy costs are about equal at $[H_2O]$ near 5×10^{17} cm^{-3}, due to the similarity of the molecular structure changes of these two processes. For the two termolecular processes involving 1H_2O [NH_3 + H_2O (H_2O catalyzed) and H_2O + NH_3 (NH_3 catalyzed)], their entropy costs are also quite similar. Note that the difference in entropy costs between a bimolecular process and its catalyzed variant is about 11 kcal mol^{-1} if the concentration of the catalyst (H_2O or NH_3) is 5×10^{17} cm^{-3}. Thus, for such a termolecular process to be competitive under this condition, its energy gain (lowering in ΔE_0) has to be greater than 11 kcal mol^{-1}. Here we chose $[H_2O] = 5 \times 10^{17}$ cm^{-3} (RH is 65% at 298 K) as a representative condition of a medium-high humidity.

As will be shown below, a great advantage of this analysis is that the variation of the entropy cost is quite predictable for the considered reactions.

Partitioning $\Delta G^{1st\text{-}ord} - \Delta E_0$: Translational, Rotational, and Vibrational Motions. For a bimolecular process from the separated reactants to the transition state, the translational degrees of freedom change from 6 to 3, the rotational ones also change from 6 to 3 (if both reactants are nonlinear molecules), and the vibrational degrees of freedom would increase by 6. We may estimate the corresponding entropy cost by assuming a rigid-rotor-harmonic-oscillator model. An example for $CH_2OO + H_2O \rightarrow$ TS is shown in Figure 8. Note that the translational partition function depends on the concentration, so does the translational part of the entropy cost.

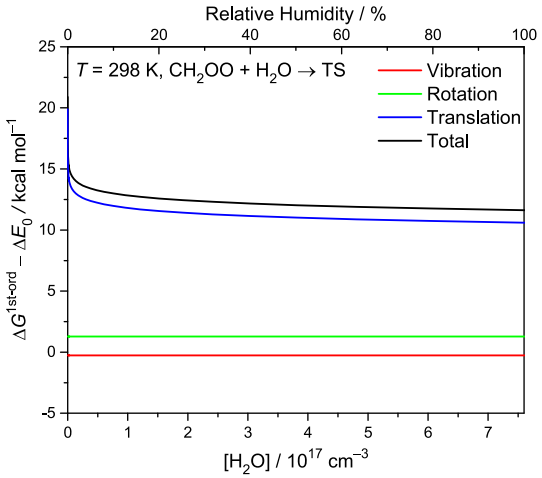

Figure 8. Entropy costs from the separated reactants to the transition state for the reaction of $CH_2OO + H_2O$ as a function of $[H_2O]$. The total entropy cost ($\Delta G^{1st\text{-}ord} - \Delta E_0$, black line) is partitioned as the contributions of the translational (blue), rotational (green), and vibrational (red) motions.

In Figure 8, we can see that the rotational contribution is small and positive, due to the compensation of the decrease in the degrees of freedom and the increase in the moments of inertia. The vibrational contribution is negative owing to the increase in the number of the vibrational modes. However, the most significant change is in the transitional degrees of freedom, which is a large increase of >11 kcal mol^{-1} (becomes larger if the concentration goes lower; see the Appendix; Figure 7 also shows a similar result). The translational partition functions only depend on simple parameters (concentration, temperature, and molecular masses) and can be easily estimated. In the case of the H_2O catalyzed reaction of *syn*-CH_3CHOO + NH_3, the translational contribution by including an additional H_2O is 11 kcal mol^{-1} at $[H_2O] = 5 \times 10^{17}$ cm^{-3}; this entropy cost would increase at lower $[H_2O]$ (by $RT\ln([H_2O]/[H_2O]^{ref})$, which is about 1.36 kcal mol^{-1} for $[H_2O]/[H_2O]^{ref} = 10^{-1}$).

Figure 9 shows the rotational and vibrational entropy costs for the considered reactions, obtained from the corresponding partition functions. We can see that the rotational and vibrational contributions are very similar for different Criegee intermediates, suggesting that the calculation for one representative Criegee intermediate will be enough. In addition, the magnitudes of both the rotational and vibrational contributions correlate very well with the complexity of the coreactants ($H_2O \cong NH_3 < CH_3OH$). Furthermore, we can see that for a given reaction, the positive rotational contributions could be compensated by the negative vibra-

DOI: 10.1021/acs.jpca.9b07117
J. Phys. Chem. A 2019, 123, 8336−8348

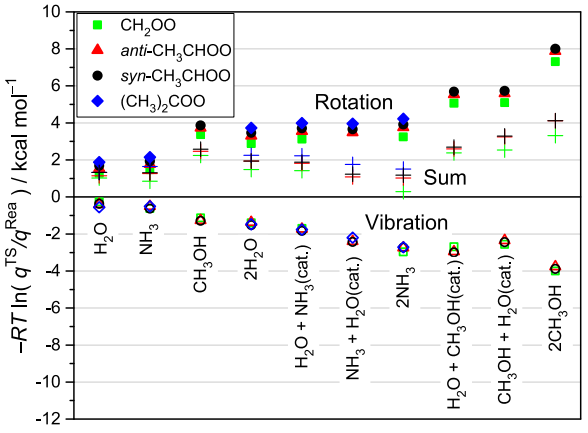

Figure 9. Rotational (solid symbol) and vibrational (open symbol) entropy costs of the reactions of Criegee intermediates (CH_2OO, green; *anti*-CH_3CHOO, red; *syn*-CH_3CHOO, black; $(CH_3)_2COO$, blue) with H_2O, NH_3, CH_3OH, and their catalysis variants. $\Delta G - \Delta E_0 = -RT\ln(q^{TS}/q^{Rea})$, where q^{TS} is the corresponding partition function of the TS and q^{Rea} means the product of the corresponding partition functions of the involved reactants. See the Appendix. The "sum" (+ symbol) means the sum of the rotational and vibrational parts. Results are from the geometries and harmonic frequencies calculated by B3LYP/6-311+G(2d,2p).

tional contribution. As a result, for the H_2O catalyzed reactions of *syn*-CH_3CHOO with NH_3, H_2O, and CH_3OH, the rovibrational contributions only account for ca. −1%, +5%, and +6%, respectively, of the differences between ($\Delta G^{1st\text{-}ord} - \Delta E_0$) of the catalyzed and bare reactions, if $[H_2O] = 5 \times 10^{17}$ cm^{-3} (the translational part is +11 kcal mol^{-1}). As the translation part increases at lower $[H_2O]$, the importance of the rovibrational parts would become smaller.

For the above H-bonding mediated reactions, the transition states of the bare reactions and the catalyzed reactions have similar structures, especially for the Criegee intermediate moiety (Figure 4). As a result, their overall rovibrational partition functions are similar, and the changes of the entropy costs are mainly governed by the translational motions. This assumption would be good, especially when these transition states are strongly H-bonded, which cause the newly formed vibrational modes to be more rigid. Indeed, the OO distances for the Criegee intermediate reactions involving H_2O and CH_3OH at the transition states are ca. 2.5 Å, significantly shorter than the OO distances in the dimers of H_2O and CH_3OH (~2.9 Å). See Table S4.

As mentioned above and indicated in Figure 5, the reactions of *syn*-CH_3CHOO + $2H_2O$ and *syn*-CH_3CHOO + $2NH_3$ are too slow to measure. Their TS energies are −6.3 and −4.5 kcal mol^{-1}, respectively. After adding the entropy costs of about 11 kcal mol^{-1} (at $[NH_3]$ or $[H_2O] = 5 \times 10^{17}$ cm^{-3}) their "effective" or "bimolecular-like" barriers become +5 and +7 kcal mol^{-1}, similar in magnitude as those of *syn*-CH_3CHOO + H_2O and $(CH_3)_2COO$ + H_2O reactions, which have not been observed either.

V. COMPETITION BETWEEN BIMOLECULAR AND TERMOLECULAR PROCESSES

CH_2OO Reaction with H_2O or NH_3 Vapor. Figure 10 (upper panel) shows the energy and free energy diagrams for the CH_2OO + H_2O and CH_2OO + $2H_2O$ reactions. For this system, the latter reaction predominates under near ambient

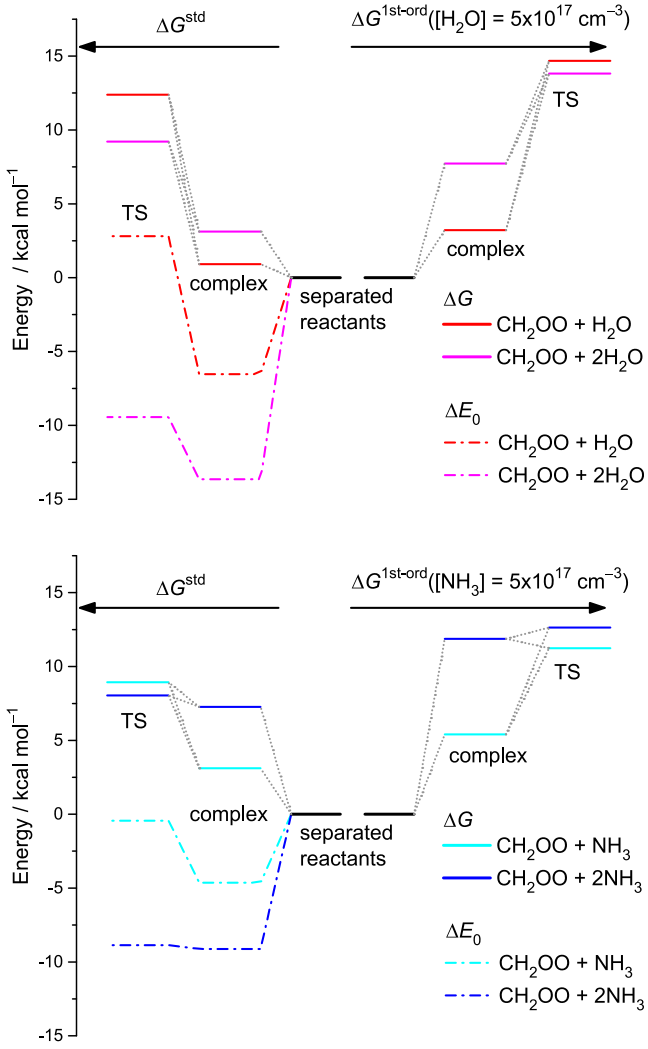

Figure 10. Diagrams of the energy ΔE, standard free energy ΔG^{std}, and pseudo-first-order free energy $\Delta G^{1st\text{-}ord}$ of the reaction of CH_2OO with water vapor (upper panel) and ammonia (lower panel) at 298 K. For both reaction systems, the ΔE barrier of the termolecular reaction is lower than that of the bimolecular reaction due to the stabilization of the extra hydrogen bonding. On the $\Delta G^{1st\text{-}ord}$ landscape, the reactions with $2H_2O$ and $1NH_3$ have the lowest barriers. Notably, the standard free energy of the TS of CH_2OO + $2NH_3$ reaction is lower than that of CH_2OO + NH_3.

conditions (298 K, $[H_2O] \geq 2 \times 10^{16}$ cm^{-3}). Analogous diagrams for the CH_2OO + NH_3 and CH_2OO + $2NH_3$ reactions are shown in Figure 10 (lower panel), for which the CH_2OO + NH_3 reaction predominates under laboratory conditions (298 K and $[NH_3] \leq 5 \times 10^{17}$ cm^{-3}). By merely looking at the ΔE or ΔG^{std} diagrams, it is not easy to see why the bimolecular process would predominate in the NH_3 reaction system as the TS level of the $2NH_3$ reaction is lower than that of the $1NH_3$ reaction in both ΔE and ΔG^{std} diagrams. The ΔE diagram does not include the entropy effect at all, but the ΔG^{std} diagram underestimates the entropy cost at TS, especially for the $2NH_3$ reaction (in this case, the used $[NH_3]$ is 5×10^{17} cm^{-3}, much less than that at 1 bar, $n^\circ = 2.4 \times 10^{19}$ cm^{-3}). By using the $\Delta G^{1st\text{-}ord}$ diagrams, we can clearly see that the ordering of the TS locations is consistent with the observed trend of reactivity.

DOI: 10.1021/acs.jpca.9b07117
J. Phys. Chem. A 2019, 123, 8336−8348

VI. OTHER WATER-MEDIATED REACTIONS

Quantum chemistry calculation shows that the gas-phase hydrolysis of carbonyl compounds has high barriers for bimolecular processes. For example, the TS energy of the reaction $H_2CO + H_2O \rightarrow CH_2(OH)_2$ is about 35.6 kcal mol^{-1}.[62] Adding one more H_2O molecule would greatly reduce the TS energy by about 22.6 kcal mol^{-1}. Therefore, the enhancement by this second water molecule will be huge, if these reactions can be measured. However, this barrier is still too high for the process to be significant.[62] Wolfe et al. has noted that even three water molecules are unable to reduce the barrier sufficiently to make the reaction feasible under atmospheric conditions.[63]

A similar case has been found for the hydrolysis reaction of glyoxal $(HCO)_2$. Quantum chemistry calculations show that the TS energy of $(HCO)_2 + 2H_2O$ is about 12 kcal mol^{-1}.[64] However, considering the entropy cost, the effective barrier is ca. 23 kcal mol^{-1} at $[H_2O] = 5 \times 10^{17}$ cm^{-3}, implying that the reaction may not be significant in the gas phase.

Turning to radical abstraction reactions, for the reaction of CH_3OH with OH radicals, the TS energies are 0.63 and −6.33 kcal mol^{-1} for the bare and water-catalyzed processes, respectively.[65] Thus, the energy gain by adding one water molecule is 7 kcal mol^{-1}, which is significantly smaller than the entropy cost (~11 kcal mol^{-1} at $[H_2O] = 5 \times 10^{17}$ cm^{-3}). A direct kinetic experiment has been performed and found that the catalysis effect of water is negligible.[65]

For the hydrolysis of SO_3, Kolb et al.[34] measured the reaction kinetics and found that the reaction rate depends on $[H_2O]$ quadratically, indicating the participation of two water molecules.[34,35] Later theoretical works also confirmed the catalytic role of the additional water molecule.[36] The TS energy of the $SO_3 + 1H_2O$ process is 19 kcal mol^{-1} while adding the second water molecule decreases the TS energy by about 27.5 kcal mol^{-1}, which easily overcomes the entropy effect and results in a low TS energy (−8.5 kcal mol^{-1}) for the $SO_3 + 2H_2O$ process.[36]

VII. REMAINING CHALLENGES

Before ending, we discuss issues and challenges remaining in quantifying H-bonding mediated reactions. First, we have considered harmonic oscillator to model the vibrational partition functions, but some systems may have large amplitude anharmonic vibrations, which may change the picture given by the rigid-rotor harmonic-oscillator model.

Also, in all the analysis above, we have assumed equilibrium between the TS and the reactants, and obtained reaction rates based on transition state theory. However, we have not clarified the dynamical pathway(s) of the reaction. To put this problem in perspective, we show the free energy landscape for two bimolecular processes and four termolecular processes of *syn*-CH_3CHOO at $[NH_3] = [H_2O] = 5 \times 10^{17}$ cm^{-3} in Figure 11. The most stable minimum is still the fully separated reactants (even at such high $[NH_3]$ and $[H_2O]$); the next stable one is *syn*-$CH_3CHOO{\cdot}H_2O$ and then *syn*-$CH_3CHOO{\cdot}(H_2O)_2$. However, the lowest effective TS is the one for the reaction of *syn*-$CH_3CHOO + NH_3 + H_2O$(cat.). Considering this termolecular reaction, a direct three-body collision is unlikely to occur. If there are no barriers between the separated reactants and the various H-bonding prereactive complexes, fast shuffle among the different prereactive complexes is expected. For the complex *syn*-$CH_3CHOO{\cdot}NH_3{\cdot}H_2O$(cat.),

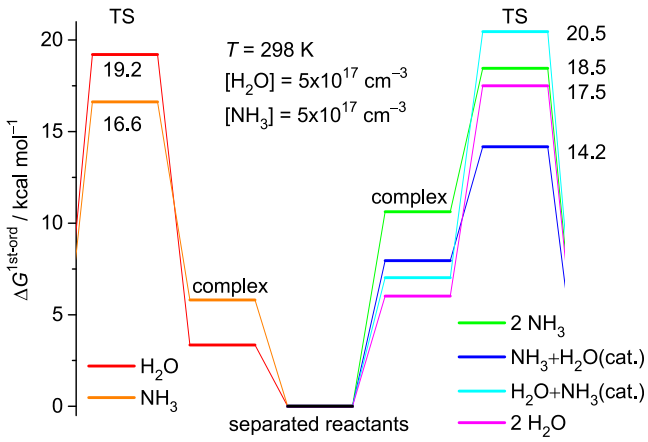

Figure 11. Free energy landscape of the bimolecular and termolecular reactions involving *syn*-CH_3CHOO, NH_3, and H_2O at $[NH_3] = [H_2O] = 5 \times 10^{17}$ cm^{-3}. The lowest barrier reaction is *syn*-$CH_3CHOO + NH_3 + H_2O$(cat.).

which is connected to the lowest effective TS, it would have a good probability to go over the TS and form the products. However, we cannot rule out the probabilities from the binary collisions of *syn*-$CH_3CHOO{\cdot}NH_3 + H_2O$ and *syn*-$CH_3CHOO{\cdot}H_2O + NH_3$ to reach the lowest transition state on the $\Delta G^{1st\text{-}ord}$ surface. More elaboration of this issue considering the encounter of a bound dimer with the third reactant molecule can be found in Supporting Information. Nonetheless, we may rule out the probability for the binary collision of *syn*-$CH_3CHOO + NH_3{\cdot}(H_2O)$ to reach the most reactive transition state. This is because the most stable 1:1 complex between H_2O and NH_3, has a configuration of H_2O donating a proton to NH_3, $HO{-}H{\cdots}NH_3$; however, the TS of the lowest barrier (Figure 4D) has the opposite configuration $H_2N{-}H{\cdots}OH_2$.[33] In addition, the reaction may also have pressure effects that will divert from the equilibrium approximation used to plot Figure 11.

Lastly, the present discussion is only for gas phase reactions, investigation on reactions in condensed phases and on interfaces is another challenge. In aqueous solutions, the hydration of reactants and the corresponding changes of solvent orientations may be more significant factors to affect the reactivity,[66−68] while the entropy cost to bring the reactants and solvent molecules together is less significant compared to that in the gas phase.

VIII. CONCLUDING REMARKS

We have demonstrated that the additional entropy cost from a bimolecular reaction to its termolecular variant is substantial and predominated by the contribution of the translational motions. The translational partition function and the corresponding entropy cost only depend on simple parameters like masses, concentrations, and temperature and can be easily estimated.

If one knows the transition state energies of a bimolecular reaction and its termolecular variant, just adding the translational entropy cost may have accounted for most of the free energy change. The remaining rovibrational parts may only contribute a minor amount (see Figures 8 and 9), depending on the complexity of the coreactants. If one requires a better accuracy, one may further calculate the rotational and vibrational partition functions for a model system consisting of

DOI: 10.1021/acs.jpca.9b07117
J. Phys. Chem. A 2019, 123, 8336−8348

CH_2OO and the coreactants. The result would be as good as the full calculations with a deviation of about 1 kcal mol^{-1}.

The success of the above approximation lies on the fact that we only need to know the difference between the transition states of the competing reactions, of which the properties including the rovibrational partition functions are quite similar. The final reactivity trend of the considered reactions mostly correlates with the TS energies after considering the entropy costs. It is noteworthy that the difference between the TS energies of the catalyzed and bare processes is less sensitive to the quantum chemistry methods. Thus, a lower-level computation would be sufficient for this issue. See Tables S2 and S3 and Figure S2 for a comparison of TS energies calculated by QCISD(T)/CBS//B3LYP/6-311+G(2d,2p) and B3LYP/6-311+G(2d,2p).

The $\Delta G^{1st\text{-}ord}$ landscape helps us to identify the lowest effective barrier which would correspond to the most favorable pathway under a given condition (temperature, reactant concentrations, etc.). As mentioned earlier, this approach is mathematically equivalent to the conventional transition state theory. We may view the present analysis as a quantitative version of the Le Chatelier principle.

APPENDIX

Transition State Theory and Free Energy

Transition state theory can be related to the free energy difference between the TS and the reactants. The example below is for a termolecular reaction, R1 + R2 + R3 → products.

$$k(T) = \frac{k_B T}{h}\frac{q^{TS}}{q^{R1}q^{R2}q^{R3}}e^{-\Delta E_0/RT} = \frac{k_B T}{h}\frac{1}{n^{\circ 2}}e^{-\Delta G^{std}/RT}$$

where $k(T)$ is the reaction rate coefficient, k_B is the Boltzmann constant, h is the Planck constant, q^{TS} and $\{q^{R1}, q^{R2}, q^{R3}\}$ are the canonical partition functions per unit volume of the TS and of the reactants {R1, R2, R3}, respectively, and ΔE_0 and ΔG^{std} are the changes of the energy E (electronic energy after vibrational zero-point correction) and the Gibbs free energy G from the reactants to the transition state at the standard conditions (P = 1 bar). n° means the concentration under standard conditions ($n^\circ = 2.43 \times 10^{19}$ cm^{-3} under 298 K by assuming ideal gas behavior).

Under a pseudo-first-order condition (given [R2] and [R3], which are much larger than [R1]) we have

$$-\frac{d[R1]}{dt} = k(T)[R1][R2][R3] = k_{eff}[R1]$$

$$\begin{aligned} k_{eff}(T) &= k(T)[R2][R3] \\ &= \frac{k_B T}{h}\frac{q^{TS}}{q^{R1}q^{R2}q^{R3}}[R2][R3]e^{-\Delta E_0/RT} \\ &= \frac{k_B T}{h}\frac{[R2]}{n^\circ}\frac{[R3]}{n^\circ}e^{-\Delta G^{std}/RT} = \frac{k_B T}{h}e^{-\Delta G^{1st-ord}/RT} \end{aligned}$$

Note that [R2] or [R3] is not necessarily at the standard condition.

Therefore, the change in Gibbs free energy under pseudo-first-order conditions can be calculated by the following equation.

$$\Delta G^{1st\text{-}ord} = \Delta E_0 - RT \ln\left(\frac{q^{TS}}{q^{R1}q^{R2}q^{R3}}[R2][R3]\right)$$

On the basis of the differential form of the Gibbs free energy, the entropy change from the reactants to the transition state is calculated.

$$\begin{aligned} T\Delta S^{1st\text{-}ord} &= -T\left(\frac{\partial \Delta G^{1st\text{-}ord}}{\partial T}\right)_P \\ &= RT \ln\left(\frac{q^{TS}}{q^{R1}q^{R2}q^{R3}}[R2][R3]\right) + \Delta E_{th}(T) \end{aligned}$$

where $\Delta E_{th}(T)$ is the change of thermal energy from the reactants to the transition state. Finally, the change of enthalpy could be calculated by following equation.

$$\Delta H^{1st\text{-}ord} = \Delta G^{1st\text{-}ord} + T\Delta S^{1st-ord} = \Delta E_0 + \Delta E_{th}$$

Absolute Magnitude of Thermal Energy, ΔE_{th}

The thermal energy difference from the reactants to TS, ΔE_{th}, could be estimated by calculating the partition functions against temperature. ΔE_{th}(298 K) is −1.2, −1.0, and +1.4 kcal mol^{-1} for the reactions of CH_2OO + NH_3, *syn*-CH_3CHOO + NH_3 + H_2O(cat.), and *syn*-CH_3CHOO + $2CH_3OH$, respectively. The negative value suggests the newly formed vibrational modes at TS are not fully activated at 298 K. For the reaction involving CH_3OH, a few low frequency vibrational modes are newly formed at TS, due to the internal rotation of the CH_3 group(s).

Gibbs Free Energy at a Given Pressure

The molar Gibbs free energy of a gaseous species at a given pressure P can be deduced with the following equation (i.e., assuming ideal gas behavior).

$$G(P) - G(P^{std}) = RT \ln(P/P^{std})$$

where $P^{std} \equiv 1$ bar $\cong$ 750 Torr.

For example, the above difference is about 2.0 kcal mol^{-1} if P = 23.8 Torr (saturated water vapor pressure at 298 K, RH = 100%), 4.8 kcal mol^{-1} for P = 0.238 Torr (RH = 1%). This is a significant amount of energy when discussing a typical chemical reaction at near ambient temperature.

ASSOCIATED CONTENT

Supporting Information

The Supporting Information is available free of charge on the ACS Publications website at DOI: 10.1021/acs.jpca.9b07117.

Discussion for picturing a termolecular reaction as a bimolecular reaction between a dimeric reactant complex and the third reactant; energy diagrams and correlation of the transition state energy differences (Figures S1 and S2); ZPE-corrected energies, transition state energy differences, OO distances, rotational temperatures, and vibrational frequencies (Tables S1−S10) (PDF)

AUTHOR INFORMATION

Corresponding Author

*Email: jimlin@gate.sinica.edu.tw.

ORCID

Kaito Takahashi: 0000-0003-2339-4295

Jim Jr-Min Lin: 0000-0002-8308-2552

Notes

The authors declare no competing financial interest.

DOI: 10.1021/acs.jpca.9b07117
J. Phys. Chem. A 2019, 123, 8336−8348

Biographies

Wen Chao obtained his Bachelor and Master degrees in Chemistry from National Taiwan University. He studied the kinetics of Criegee intermediates under the direction of Dr. Jim Jr-Min Lin at Institute of Atomic and Molecular Sciences (IAMS), Academia Sinica, Taiwan. He will start to pursue his Ph.D. degree in Chemistry at Caltech in September 2019.

Cangtao Yin obtained his Ph.D. degree at Tianjin University, focused on the reaction rate theories including transition state theory, collision theory, etc., in the framework of statistical mechanics. He joined IAMS as a postdoc under the guidance of Dr. Kaito Takahashi, studying quantum chemistry, with an emphasis on the Criegee intermediate related reactions under the atmospheric conditions.

Kaito Takahashi is a Japanese theoretical chemist, who obtained his Ph.D. from Keio University under the tutelage of Prof. Satoshi Yabushita. After four years of postdoctoral fellow research under Prof. Rex T. Skodje, he started his lab at IAMS in 2009. He is presently working as an associate research fellow there. His scientific interest for the past few years has been to understand properties that control gas phase reactions.

Jim Jr-Min Lin received his Ph.D. degree under the direction of Yuan T. Lee at National Taiwan University studying reactive scattering with crossed molecular beams. He then joined IAMS and is currently a research fellow in IAMS and an adjunct professor in the Department of Chemistry, National Taiwan University. His research experiences and interests include reactive scattering using crossed molecular beams, photodissociation, spectroscopy, and kinetics that are relevant in fundamental understanding and in atmospheric chemistry. Recent research focus is on the spectroscopy and kinetics of Criegee intermediates.

■ ACKNOWLEDGMENTS

This work is supported by Academia Sinica (AS-CDA-106-M05) and the Ministry of Science and Technology, Taiwan (MOST 107-2113-M-001-002 and MOST 106-2113-M-001-026-MY3).

■ REFERENCES

(1) Criegee, R. Mechanism of Ozonolysis. *Angew. Chem., Int. Ed. Engl.* **1975**, *14* (11), 745−752.
(2) Welz, O.; Savee, J. D.; Osborn, D. L.; Vasu, S. S.; Percival, C. J.; Shallcross, D. E.; Taatjes, C. A. Direct Kinetic Measurement of Criegee Intermediat (CH_2OO) Formed by Reaction of CH_2I with O_2. *Science* **2012**, *335* (6065), 204−207.
(3) Welz, O.; Eskola, A. J.; Sheps, L.; Rotavera, B.; Savee, J. D.; Scheer, A. M.; Osborn, D. L.; Lowe, D.; Murray Booth, A.; Xiao, P. Rate Coefficients of C1 and C2 Criegee Intermediate Reactions with Formic and Acetic Acid near the Collision Limit: Direct Kinetics Measurements and Atmospheric Implications. *Angew. Chem., Int. Ed.* **2014**, *53* (18), 4547−4550.
(4) Chao, W.; Hsieh, J. T.; Chang, C. H.; Lin, J. J. Direct Kinetic Measurement of the Reaction of the Simplest Criegee Intermediate with Water Vapor. *Science* **2015**, *347* (6223), 751−754.
(5) Foreman, E. S.; Kapnas, K. M.; Murray, C. Reactions between Criegee Intermediates and the Inorganic Acids HCl and HNO_3: Kinetics and Atmospheric Implications. *Angew. Chem., Int. Ed.* **2016**, *55* (35), 10419−10422.
(6) Taatjes, C. A. Criegee Intermediates: What Direct Production and Detection Can Teach Us About Reactions of Carbonyl Oxides. *Annu. Rev. Phys. Chem.* **2017**, *68* (1), 183−207.
(7) Lin, J. J.; Chao, W. Structure-Dependent Reactivity of Criegee Intermediates Studied with Spectroscopic Methods. *Chem. Soc. Rev.* **2017**, *46* (24), 7483−7497.
(8) Osborn, D. L.; Taatjes, C. A. The Physical Chemistry of Criegee Intermediates in the Gas Phase. *Int. Rev. Phys. Chem.* **2015**, *34* (3), 309−360.
(9) Su, Y.-T.; Huang, Y.-H.; Witek, H. A.; Lee, Y.-P. Infrared Absorption Spectrum of the Simplest Criegee Intermediate CH_2OO. *Science* **2013**, *340*, 174−176.
(10) Li, J.; Carter, S.; Bowman, J. M.; Dawes, R.; Xie, D.; Guo, H. High-Level, First-Principles, Full-Dimensional Quantum Calculation of the Ro-Vibrational Spectrum of the Simplest Criegee Intermediate (CH_2OO). *J. Phys. Chem. Lett.* **2014**, *5* (13), 2364−2369.
(11) Taatjes, C. A.; Welz, O.; Eskola, A. J.; Savee, J. D.; Scheer, A. M.; Shallcross, D. E.; Rotavera, B.; Lee, E. P. F.; Dyke, J. M.; Mok, D. K. W. Direct Measurements of Conformer-Dependenct Reactivity of the Criegee Intermediate CH_3CHOO. *Science* **2013**, *340* (6129), 177−180.
(12) Smith, M. C.; Chang, C. H.; Chao, W.; Lin, L. C.; Takahashi, K.; Boering, K. A.; Lin, J. J. Strong Negative Temperature Dependence of the Simplest Criegee Intermediate CH_2OO Reaction with Water Dimer. *J. Phys. Chem. Lett.* **2015**, *6* (14), 2708−2713.
(13) Lin, L.-C.; Chao, W.; Chang, C.-H.; Takahashi, K.; Lin, J. J. Temperature Dependence of the Reaction of *anti*-CH_3CHOO with Water Vapor. *Phys. Chem. Chem. Phys.* **2016**, *18* (40), 28189−28197.
(14) Sheps, L.; Scully, A. M.; Au, K. UV Absorption Probing of the Conformer-Dependent Reactivity of a Criegee Intermediate CH_3CHOO. *Phys. Chem. Chem. Phys.* **2014**, *16* (48), 26701−26706.
(15) Huang, H.-L.; Chao, W.; Lin, J. J. Kinetics of a Criegee Intermediate That Would Survive High Humidity and May Oxidize Atmospheric SO_2. *Proc. Natl. Acad. Sci. U. S. A.* **2015**, *112* (35), 10857−10862.
(16) Smith, M. C.; Chao, W.; Takahashi, K.; Boering, K. A.; Lin, J. J. Unimolecular Decomposition Rate of the Criegee Intermediate $(CH_3)_2COO$ Measured Directly with UV Absorption Spectroscopy. *J. Phys. Chem. A* **2016**, *120* (27), 4789−4798.
(17) Lester, M. I.; Klippenstein, S. J. Unimolecular Decay of Criegee Intermediates to OH Radical Products: Prompt and Thermal Decay Processes. *Acc. Chem. Res.* **2018**, *51* (4), 978−985.
(18) Vereecken, L.; Novelli, A.; Taraborrelli, D. Unimolecular Decay Strongly Limits the Atmospheric Impact of Criegee Intermediates. *Phys. Chem. Chem. Phys.* **2017**, *19* (47), 31599−31612.
(19) Yin, C.; Takahashi, K. How Does Substitution Affect the Unimolecular Reaction Rates of Criegee Intermediates? *Phys. Chem. Chem. Phys.* **2017**, *19* (19), 12075−12084.
(20) Taatjes, C. A.; Shallcross, D. E.; Percival, C. J. Research Frontiers in the Chemistry of Criegee Intermediates and Tropospheric Ozonolysis. *Phys. Chem. Chem. Phys.* **2014**, *16* (5), 1704−1718.
(21) Lee, Y. P. Perspective: Spectroscopy and Kinetics of Small Gaseous Criegee Intermediates. *J. Chem. Phys.* **2015**, *143* (2), 020901.
(22) Kumar, M.; Sinha, A.; Francisco, J. S. Role of Double Hydrogen Atom Transfer Reactions in Atmospheric Chemistry. *Acc. Chem. Res.* **2016**, *49* (5), 877−883.
(23) Buszek, R. J.; Francisco, J. S.; Anglada, J. M. Water Effects on Atmospheric Reactions. *Int. Rev. Phys. Chem.* **2011**, *30* (3), 335−369.
(24) Aloisio, S.; Francisco, J. S. Radical-Water Complexes in Earth's Atmosphere. *Acc. Chem. Res.* **2000**, *33* (12), 825−830.
(25) Vaida, V. Perspective: Water Cluster Mediated Atmospheric Chemistry. *J. Chem. Phys.* **2011**, *135*, 020901.
(26) Thomsen, D. L.; Kurtén, T.; Jorgensen, S.; Wallington, T. J.; Baggesen, S. B.; Aalling, C.; Kjaergaard, H. G. On the Possible Catalysis by Single Water Molecules of Gas-Phase Hydrogen Abstraction Reactions by OH Radicals. *Phys. Chem. Chem. Phys.* **2012**, *14* (37), 12992−12999.
(27) Liu, J.; Fang, S.; Liu, W.; Wang, M.; Tao, F. M.; Liu, J. Y. Mechanism of the Gaseous Hydrolysis Reaction of SO_2: Effects of NH_3versus H_2O. *J. Phys. Chem. A* **2015**, *119* (1), 102−111.
(28) Li, H.; Zhong, J.; Vehkamäki, H.; Kurtén, T.; Wang, W.; Ge, M.; Zhang, S.; Li, Z.; Zhang, X.; Francisco, J. S. Self-Catalytic Reaction of SO_3 and NH_3 to Produce Sulfamic Acid and Its

DOI: 10.1021/acs.jpca.9b07117
J. Phys. Chem. A 2019, 123, 8336−8348

Implication to Atmospheric Particle Formation. *J. Am. Chem. Soc.* **2018**, *140* (35), 11020−11028.
(29) Gonzalez, J.; Anglada, J. M.; Buszek, R. J.; Francisco, J. S. Impact of Water on the OH + HOCl Reaction. *J. Am. Chem. Soc.* **2011**, *133* (10), 3345−3353.
(30) Bandyopadhyay, B.; Kumar, P.; Biswas, P. Ammonia Catalyzed Formation of Sulfuric Acid in Troposphere: The Curious Case of a Base Promoting Acid Rain. *J. Phys. Chem. A* **2017**, *121* (16), 3101−3108.
(31) Vöhringer-Martinez, E.; Hansmann, B.; Hernandez, H.; Francisco, J. S.; Troe, J.; Abel, B. Water Catalysis of a Radical-Molecule Gas-Phase Reaction. *Science* **2007**, *315* (5811), 497−501.
(32) Lin, Y.-H.; Yin, C.; Lin, W.-H.; Li, Y.-L.; Takahashi, K.; Lin, J. J. Criegee Intermediate Reaction with Alcohol Is Enhanced by a Single Water Molecule. *J. Phys. Chem. Lett.* **2018**, *9*, 7040−7044.
(33) Chao, W.; Yin, C.; Li, Y. L.; Takahashi, K.; Lin, J. J. Synergy of Water and Ammonia Hydrogen Bonding in a Gas-Phase Reaction. *J. Phys. Chem. A* **2019**, *123* (7), 1337−1342.
(34) Kolb, C. E.; Jayne, J. T.; Worsnop, D. R.; Molina, M. J.; Meads, R. F.; Viggiano, A. A. Gas Phase Reaction of Sulfur Trioxide with Water Vapor. *J. Am. Chem. Soc.* **1994**, *116* (22), 10314−10315.
(35) Lovejoy, E. R.; Hanson, D. R.; Huey, L. G. Kinetics and Products of the Gas-Phase Reaction of SO_3 with Water. *J. Phys. Chem.* **1996**, *100* (51), 19911−19916.
(36) Loerting, T.; Liedl, K. R. Toward Elimination of Discrepancies between Theory and Experiment: The Rate Constant of the Atmospheric Conversion of SO_3 to H_2SO_4. *Proc. Natl. Acad. Sci. U. S. A.* **2000**, *97* (16), 8874−8878.
(37) Ryzhkov, A. B.; Ariya, P. A. Theoretical Study of the Reactions of Parent and Substituted Criegee Intermediates with Water and the Water Dimer. *Phys. Chem. Chem. Phys.* **2004**, *6* (21), 5042−5050.
(38) Lin, L. C.; Chang, H. T.; Chang, C. H.; Chao, W.; Smith, M. C.; Chang, C. H.; Lin, J. J.; Takahashi, K. Competition between H_2O and $(H_2O)_2$ Reactions with CH_2OO/CH_3CHOO. *Phys. Chem. Chem. Phys.* **2016**, *18* (6), 4557−4568.
(39) Anglada, J. M.; Solé, A. Impact of the Water Dimer on the Atmospheric Reactivity of Carbonyl Oxides. *Phys. Chem. Chem. Phys.* **2016**, *18* (26), 17698−17712.
(40) Sheps, L.; Rotavera, B.; Eskola, A. J.; Osborn, D. L.; Taatjes, C. A.; Au, K.; Shallcross, D. E.; Khan, M. A. H.; Percival, C. J. The Reaction of Criegee Intermediate CH_2OO with Water Dimer: Primary Products and Atmospheric Impact. *Phys. Chem. Chem. Phys.* **2017**, *19* (33), 21970−21979.
(41) Ryzhkov, A. B.; Ariya, P. A. The Importance of Water Clusters $(H_2O)_n$ (n = 2, ..., 4) in the Reaction of Criegee Intermediate with Water in the Atmosphere. *Chem. Phys. Lett.* **2006**, *419* (4−6), 479−485.
(42) Ewing, M. B.; Lilley, T. H.; Olofsson, G. M.; Ratzsch, M. T.; Somsen, G. Standard Quantities in Chemical Thermodynamics. Fugacities, Activities and Equilibrium Constants for Pure and Mixed Phases. (IUPAC Recommendations). *Pure Appl. Chem.* **1994**, *66* (3), 533−552.
(43) Lin, L. C.; Takahashi, K. Will $(CH_3)_2COO$ Survive in Humid Conditions? *J. Chin. Chem. Soc.* **2016**, *63* (6), 472−479.
(44) Long, B.; Bao, J. L.; Truhlar, D. G. Atmospheric Chemistry of Criegee Intermediates: Unimolecular Reactions and Reactions with Water. *J. Am. Chem. Soc.* **2016**, *138* (43), 14409−14422.
(45) Berndt, T.; Kaethner, R.; Voigtländer, J.; Stratmann, F.; Pfeifle, M.; Reichle, P.; Sipilä, M.; Kulmala, M.; Olzmann, M. Kinetics of the Unimolecular Reaction of CH_2OO and the Bimolecular Reactions with the Water Monomer, Acetaldehyde and Acetone under Atmospheric Conditions. *Phys. Chem. Chem. Phys.* **2015**, *17* (30), 19862−19873.
(46) Liu, Y.; Yin, C.; Smith, M. C.; Liu, S.; Chen, M.; Zhou, X.; Xiao, C.; Dai, D.; Lin, J. J.; Takahashi, K. Kinetics of the Reaction of the Simplest Criegee Intermediate with Ammonia: A Combination of Experiment and Theory. *Phys. Chem. Chem. Phys.* **2018**, *20* (47), 29669−29676.
(47) Misiewicz, J. P.; Elliott, S. N.; Moore, K. B.; Schaefer, H. F. Re-Examining Ammonia Addition to the Criegee Intermediate: Converging to Chemical Accuracy. *Phys. Chem. Chem. Phys.* **2018**, *20* (11), 7479−7491.
(48) Chhantyal-Pun, R.; Shannon, R. J.; Tew, D. P.; Caravan, R. L.; Duchi, M.; Wong, C.; Ingham, A.; Feldman, C.; McGillen, M. R.; Khan, M. A. H. Experimental and Computational Studies of Criegee Intermediate Reactions with NH_3 and CH_3NH_2. *Phys. Chem. Chem. Phys.* **2019**, *21*, 14042−14052.
(49) McGillen, M. R.; Curchod, B. F. E.; Chhantyal-Pun, R.; Beames, J. M.; Watson, N.; Khan, M. A. H.; McMahon, L.; Shallcross, D. E.; Orr-Ewing, A. J. Criegee Intermediate-Alcohol Reactions, A Potential Source of Functionalized Hydroperoxides in the Atmosphere. *ACS Earth Sp. Chem.* **2017**, *1* (10), 664−672.
(50) Chao, W.; Lin, Y.-H.; Yin, C.; Lin, W.-H.; Takahashi, K.; Lin, J. J. Temperature and Isotope Effects in the Reaction of CH_3CHOO with Methanol. *Phys. Chem. Chem. Phys.* **2019**, *21* (25), 13633−13640.
(51) Watson, N. A. I.; Black, J. A.; Stonelake, T. M.; Knowles, P. J.; Beames, J. M. An Extended Computational Study of Criegee Intermediate-Alcohol Reactions. *J. Phys. Chem. A* **2019**, *123* (1), 218−229.
(52) Tadayon, S. V.; Foreman, E. S.; Murray, C. Kinetics of the Reactions between the Criegee Intermediate CH_2OO and Alcohols. *J. Phys. Chem. A* **2018**, *122* (1), 258−268.
(53) Yin, C.; Takahashi, K. Effect of Unsaturated Substituents in the Reaction of Criegee Intermediates with Water Vapor. *Phys. Chem. Chem. Phys.* **2018**, *20* (30), 20217−20227.
(54) Greenwald, E. E.; North, S. W.; Georgievskii, Y.; Klippenstein, S. J. A Two Transition State Model for Radical-Molecule Reactions: A Case Study of the Addition of OH to C_2H_4. *J. Phys. Chem. A* **2005**, *109* (27), 6031−6044.
(55) Senosiain, J. P.; Klippenstein, S. J.; Miller, J. A. Reaction of Ethylene with Hydroxyl Radicals: A Theoretical Study. *J. Phys. Chem. A* **2006**, *110* (21), 6960−6970.
(56) Pople, J. A.; Head-Gordon, M.; Raghavachari, K. Quadratic Configuration Interaction. A General Technique for Determining Electron Correlation Energies. *J. Chem. Phys.* **1987**, *87* (10), 5968−5975.
(57) Dunning, T. H. Gaussian Basis Sets for Use in Correlated Molecular Calculations. I. The Atoms Boron through Neon and Hydrogen. *J. Chem. Phys.* **1989**, *90* (2), 1007−1023.
(58) Kendall, R. A.; Dunning, T. H.; Harrison, R. J. Electron Affinities of the First-Row Atoms Revisited. Systematic Basis Sets and Wave Functions. *J. Chem. Phys.* **1992**, *96* (9), 6796−6806.
(59) Dunning, J.; Peterson, K. A.; Wilson, A. K. Gaussian Basis Sets for Use in Correlated Molecular Calculations. X. The Atoms Aluminum through Argon Revisited. *J. Chem. Phys.* **2001**, *114* (21), 9244−9253.
(60) Becke, A. D. Density-Functional Thermochemistry. III. The Role of Exact Exchange. *J. Chem. Phys.* **1993**, *98* (7), 5648−5652.
(61) Krishnan, R.; Binkley, J. S.; Seeger, R.; Pople, J. A. Self-Consistent Molecular Orbital Methods. XX. A Basis Set for Correlated Wave Functions. *J. Chem. Phys.* **1980**, *72* (1), 650−654.
(62) Hazra, M. K.; Francisco, J. S.; Sinha, A. Gas Phase Hydrolysis of Formaldehyde to Form Methanediol: Impact of Formic Acid Catalysis. *J. Phys. Chem. A* **2013**, *117* (46), 11704−11710.
(63) Wolfe, S.; Kim, C. K.; Yang, K.; Weinberg, N.; Shi, Z. Hydration of the Carbonyl Group. A Theoretical Study of the Cooperative Mechanism. *J. Am. Chem. Soc.* **1995**, *117* (15), 4240−4260.
(64) Hazra, M. K.; Francisco, J. S.; Sinha, A. Hydrolysis of Glyoxal in Water-Restricted Environments: Formation of Organic Aerosol Precursors through Formic Acid Catalysis. *J. Phys. Chem. A* **2014**, *118* (23), 4095−4105.
(65) Chao, W.; Lin, J. J.; Takahashi, K.; Tomas, A.; Yu, L.; Kajii, Y.; Batut, S.; Schoemaecker, C.; Fittschen, C. Water Vapor Does Not Catalyze the Reaction between Methanol and OH Radicals. *Angew. Chem., Int. Ed.* **2019**, *58* (15), 5013−5017.

DOI: 10.1021/acs.jpca.9b07117
J. Phys. Chem. A 2019, 123, 8336−8348

(66) Zhong, J.; Kumar, M.; Zhu, C. Q.; Francisco, J. S.; Zeng, X. C. Surprising Stability of Larger Criegee Intermediates on Aqueous Interfaces. *Angew. Chem., Int. Ed.* **2017**, *56* (27), 7740−7744.
(67) Zhong, J.; Kumar, M.; Francisco, J. S.; Zeng, X. C. Insight into Chemistry on Cloud/Aerosol Water Surfaces. *Acc. Chem. Res.* **2018**, *51* (5), 1229−1237.
(68) Kumar, M.; Zhong, J.; Zeng, X. C.; Francisco, J. S. Reaction of Criegee Intermediate with Nitric Acid at the Air-Water Interface. *J. Am. Chem. Soc.* **2018**, *140* (14), 4913−4921.

DOI: 10.1021/acs.jpca.9b07117
J. Phys. Chem. A 2019, 123, 8336−8348